

Hop Constrained Steiner Trees with multiple Root Nodes

Luis Gouveia, Markus Leitner, Ivana Ljubić

Forschungsbericht / Technical Report

TR-186-1-13-02

April 8, 2013



Hop Constrained Steiner Trees with multiple Root Nodes

Luis Gouveia^{a,1}, Markus Leitner^{b,2,*}, Ivana Ljubić^{c,3}

^a*DEIO/CIO Faculdade de Ciências, Universidade de Lisboa, Bloco C2, Campo Grande, 1749-016, Lisboa, Portugal*

^b*Institute of Computer Graphics and Algorithms, Vienna University of Technology, Favoritenstraße 9-11, 1040 Vienna, Austria*

^c*Department of Statistics and Operations Research, University of Vienna, Brünnerstraße 72, 1210 Vienna, Austria*

Abstract

We consider a network design problem that generalizes the hop and diameter constrained Steiner tree problem as follows: Given an edge-weighted undirected graph with two disjoint subsets representing *roots* and *terminals*, find a minimum-weight subtree that spans all the roots and terminals so that the number of hops between each *relevant node* and an arbitrary root does not exceed a given hop limit H . The set of relevant nodes may be equal to the set of terminals, or to the union of terminals and root nodes. This article proposes integer linear programming models utilizing one layered graph for each root node. Different possibilities to relate solutions on each of the layered graphs as well as additional strengthening inequalities are then discussed. Furthermore, theoretical comparisons between these models and to previously proposed flow- and path-based formulations are given. To solve the problem to optimality, we implement branch-and-cut algorithms for the layered graph formulations. Our computational study shows their clear advantages over previously existing approaches.

Keywords: Integer programming, OR in telecommunications, Steiner tree, Hop-constraints

*Corresponding author. Tel.:+43-1-58801-18624; Fax:+43-1-58801-18699.

Email addresses: legouveia@fc.ul.pt (Luis Gouveia), leitner@ads.tuwien.ac.at (Markus Leitner), ivana.ljubic@univie.ac.at (Ivana Ljubić)

¹Supported by the National Funding from FCT - Fundação para a Ciência e Tecnologia, under the project: PEst-OE/MAT/UI0152.

²Supported by the Austrian Science Fund (FWF) under grant I892-N23.

³Supported by the APART Fellowship of the Austrian Academy of Sciences.

1. Introduction

Quality-of-service aspects are among the major issues when designing modern telecommunication networks and in particular bounding the maximum overall delay of each relevant communication path is important. It is widely accepted that in many applications the delay along some connection mainly depends on the number of intermediate routers, i.e., hops, and that restricting the maximum length of each established path by some predefined threshold limits the probability of failures. Furthermore, whenever redundancy is not of major importance it is usually desired that the final network has tree structure in order to ensure unique communication paths. The literature contains many works dedicated to two problems that fit into this framework, namely the “centralized” hop-constrained minimum spanning/Steiner tree problem (HMSTP / HMStTP), see, e.g., [4, 6, 8, 12, 13, 20] and the references therein, and the “decentralized” diameter-constrained minimum spanning/Steiner tree problem (DMSTP / DMStTP), see, e.g., [1, 7, 9, 10, 13, 16] and the references therein.

To define the HMSTP consider an undirected, edge-weighted graph $G = (V, E)$ with node set V , edge set E , a hop limit $H \in \mathbb{N}$, and one dedicated central node $r \in V$. The objective is to identify a minimum cost spanning tree such that the path between the root r and any node $v \in V$ does consist of at most H edges. For the Steiner variant (HMStTP) we are further given a set of terminals $T \subset V$ and the aim is to identify a minimum cost Steiner tree connecting all terminals such that the path between the root r and any terminal node $t \in T$ does consist of at most H edges. To define the DMSTP consider, as before, an undirected, edge-weighted graph. The objective is to identify a minimum cost spanning tree such that the path between any two nodes does consist of at most D edges, for some given diameter limit $D \in \mathbb{N}$. Changes to the Steiner variant (DMStTP) are analogous to the hop-constrained problems.

However, several other tree problems with hop constraints appear to be of practical interest and one objective of this work is to propose a more general framework to contextualize these problems. In practice we may have multiple (e.g., replicated) central servers in which case each server communicates with a subset of terminals. Hop constraints are imposed on the communication paths, e.g., between each server-terminal pair, to ensure that the communication delays are not too high and also to ensure a certain reliability of the network, cf. [4].

Consider, thus, the general and new Hop Constrained Minimum Steiner Tree Problem with Multiple Root nodes (HSTPMR) problem. We are given an undirected graph $G = (V, E)$, with node set V , edge set E , edge costs $c_e \geq 0$, for all $e \in E$, and a hop limit $H \in \mathbb{N}$.

The node set V contains two disjoint subsets: root nodes R , $|R| \geq 1$, and terminal nodes $T \subseteq V \setminus R$. Furthermore, we are given a set $T' \subseteq T \cup R$ of *relevant nodes* for which hop limits to all root nodes need to be considered.

A solution to the HSTPMR is a Steiner tree $G' = (V', E')$ spanning all root and terminal nodes, i.e., $R \cup T \subseteq V'$, such that the hop constraints are met for all relevant nodes $v \in T'$. More precisely, for each relevant node $t \in T'$ and each root $r \in R$, the unique path between t and r can contain at most H edges. The objective is to find a feasible subtree yielding minimum total edge costs. If $T \cup R = V$, the solution will be a spanning tree of G .

In this study we consider two particular cases of this new framework which as far as we know have not been studied before (with exception to the introductory work in [14]): a) $T' = T \cup R$ and b) $T' = T$. In the first case, delay bounds between roots have to be taken into consideration (e.g., when roots model replica servers) and in the second case delays between roots are not critical (e.g., when services by different providers are offered to terminals). An illustrative instance of the HSTPMR with two roots and three terminals is given in Figure 1(a), while Figures 1(b) and 1(c) depict solutions to this instance for $T' = T \cup R$ and $T' = T$, respectively, assuming that $H = 3$. Notice that one could generalize this problem even further by introducing subsets of roots and hop limits that would depend on each node from T' .

However, the two cases already present different characteristics that strongly affect the corresponding models. For the case $T' = T \cup R$, it is easy to see that the hop-constrained arborescences associated to each root span the same set of nodes and the same set of undirected edges. This property is useful to strengthen the models that will be proposed in the next subsection. Unfortunately, this property may not be satisfied in the case $T' = T$ since the maximum distance between any two roots may exceed H . In fact as can be deduced from Figure 1(c), the subtree obtained from undirecting the arcs of the hop-constrained arborescence associated to root 0 does not coincide with the subtree obtained from undirecting the arcs of the hop-constrained arborescence associated to root 1. Thus, many of the model enhancements valid for the case $T' = T \cup R$ that we will discuss below, will not be valid for $T' = T$. The following results, however, provide an upper bound on the maximum distance between any two roots:

Lemma 1. *Let $G' = (V', E')$ be a feasible solution to an instance of the HSTPMR with $T' = T$ and let $d(u, v)$ denote the distance between two nodes $u, v \in V'$ in G' . Then, the maximum distance between any pair of root nodes in G' does not exceed $2H - \ell$ where ℓ is the maximum distance between any two terminal nodes in G' , i.e., $\ell = \max_{u, v \in T} d(u, v)$.*

Proof. If there is a single terminal, two roots can be each at distance H from it, which gives the maximum distance of $2H$. Assume that $|T| \geq 2$, let t_1 and t_2 be two terminals at maximum distance and let $P = (t_1 = v_0, v_1, \dots, v_\ell = t_2)$ ($v_i \in V'$ for $0 \leq i \leq \ell$, and $\{v_i, v_{i+1}\} \in E'$ for $0 \leq i \leq \ell - 1$) denote the path between t_1 and t_2 in G' . Furthermore, let $r \in R$ be an arbitrary root and $v_j \in P$, $0 \leq j \leq \ell$, be the node from P such that the path between r and v_j is edge disjoint to P . Since, the maximum distance between a terminal and a root node may not exceed H , we have

$$d(r, v_j) \leq \begin{cases} H - \ell + j & \text{if } j \leq \ell/2 \\ H - j & \text{if } j \geq \ell/2 \end{cases}$$

Now let $s \in R$ be another root and $v_k \in P$, $0 \leq k \leq \ell$ again be the node from P such that the path between s and v_k is edge disjoint to P . Without loss of generality we assume that $j \leq k$. Then, by case distinction it is easy to see that

$$d(r, s) = d(r, v_j) + d(v_j, v_k) + d(s, v_k) \leq 2H - \ell$$

holds and that this bound can be tight. □

The next corollary immediately follows from Lemma 1.

Corollary 1. *Let $\text{diam}(T)$ be the minimum diameter of a subtree of G spanning all nodes from T . Then, for any feasible solution $G' = (V', E')$ to an instance of the HSTPMR on G with $T' = T$ the maximum distance between any pair of root nodes in G' does not exceed H' , where $H' = 2H - \text{diam}(T)$.*

Notice that H' can be calculated in polynomial time: It suffices to run breadth-first-search starting from each $t \in T$ until all remaining terminals are reached. The subtree with the smallest diameter obtained gives us the value of $\text{diam}(T)$. As we will show in Section 3.4, this corollary allows us to provide modified models, where many of the enhancements directly valid for the case $T' = T \cup R$ apply. The drawback is that these modified models use many more variables and constraints than the original model without the enhancements.

Our Contribution. In this paper, besides introducing the general and new problem we present three kinds of results: a) Complexity: We analyze special cases in which the HSTPMR can be reduced to previously studied network design problems, identify special polynomial cases, show that the problem is NP-hard in general, and that one cannot guarantee to find an

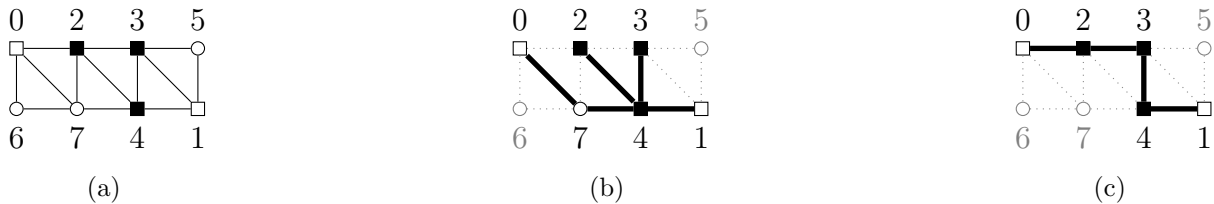


Figure 1: (a) An illustrative instance with $R = \{0, 1\}$, $T = \{2, 3, 4\}$, and potential Steiner nodes $S = \{5, 6, 7\}$. (b) A feasible solution for $T' = T \cup R$ and $H = 3$. (c) A feasible solution for $T' = T$ and $H = 3$.

approximation ratio better than $\Theta(\log |V|)$ unless $P=NP$. b) Mixed integer programming (MIP) models: We discuss layered graph reformulations, present strengthening valid inequalities and show that the obtained models theoretically dominate flow- and path-based models studied in [14]. c) Computational results: Branch-and-cut algorithms are developed for layered graph models and computationally compared to each other and to the best performing approach from [14]. Computations are carried out on a set of benchmark instances known from the HMSTP – the results show that the branch-and-cut approaches appear to be reasonable alternatives to solve these more general cases.

Outline of the Paper. In the remainder of this section we study the computational complexity of the HSTPMR. In Section 2 we discuss a generic integer linear programming (ILP) formulation of the problem and review a path-based formulation from our previous work [14] which outperformed the other flow- and path-based models from [14] both theoretically, i.e., with respect to the quality of its linear programming (LP) bounds, and computationally. Afterwards, two possibilities for reformulating the HSTPMR over layered graphs together with further valid inequalities for strengthening the LP relaxations of the resulting models are discussed in Section 3. In Section 4 we compare our models with respect to their LP relaxation values and also show which variants dominate the previously proposed models. Details of the developed branch-and-cut approaches are given in Section 5, where we also discuss the results of our computational study. Finally, some conclusions are drawn in Section 6.

1.1. Computational Complexity

Next, we analyze the computational complexity of the HSTPMR and its relationship with other problems. Obviously, for singleton sets R and T the problem becomes the Hop Constrained Shortest Path Problem (HSPP) which can be solved in polynomial time for any H since we are given nonnegative edge costs. If either $|R| = 1$ or $|T| = 1$ (but not both), the problem is either the HMStTP if $V \neq T \cup R$ or the HMSTP if $V = T \cup R$. These problems

are known to be NP-hard if $2 \leq H < |V| - 1$, cf. [6]. If $T' = R$ or $|T| = 1$ and $T' = T \cup R$, we have the DMStTP or the DMSTP with the diameter equal to H which are known to be NP hard if $4 \leq H < |V| - 1$, cf. [5].

In the remainder of this paper, we will consider the most general case, assuming that $H \geq 3$, $|R| \geq 2$ and $|T| \geq 2$, which is shown to be NP-hard by the following Lemma (see Appendix for the proof).

Lemma 2. *Assuming that $|R| \geq 2$ and $|T| \geq 2$, the HSTPMR can be solved in polynomial time for $H = 2$. For $H \geq 3$, the problem is NP-hard, and it cannot be guaranteed to find an approximation ratio better than $\Theta(\log n)$ unless $P=NP$.*

An overview on all complexity results regarding the HSTPMR and its relationships with related problems is provided in Table 1 where “ $\in P$ ” is used to denote cases when the problem is solvable in polynomial time and “–” denotes that a particular case is infeasible or that no previously considered problem corresponds to that case.

Notation. Let $S = V \setminus (T \cup R)$ denote the set of remaining nodes that we will refer to as potential Steiner nodes. To model a feasible solution $G' = (V', E')$ on G , we will use binary edge variables, x_{ij} , that are set to one if $\{i, j\} \in E'$, and to zero, otherwise, for all $\{i, j\} \in E$. In addition, we will use binary node variables associated to potential Steiner nodes: y_i is set to one if $i \in V' \cap S$, and to zero, otherwise, for all nodes $v \in S$. Furthermore, let $A = \{(i, j), (j, i) \mid \{i, j\} \in E\}$ denote the set of bi-directed arcs in G . For a subset $W \subset V$, we use $\delta(W) = \{\{i, j\} \in E \mid i \notin W, j \in W\}$, $\delta^-(W) = \{(i, j) \in A \mid i \notin W, j \in W\}$, and $\delta^+(W) = \{(i, j) \in A \mid i \in W, j \notin W\}$ to denote the undirected and directed, ingoing and outgoing cutset, respectively. For a set of arcs A' and some vector of variables \mathbf{z} , we also use notation $z[A'] = \sum_{(i,j) \in A'} z_{ij}$. Finally, for a binary vector $\mathbf{x} \in \{0, 1\}^{|E|}$ let $E(\mathbf{x})$ denote the subset of edges for which $x_e = 1$.

Table 1: Complexity of the HSTPMR.

$ R $	$ T $	T'	Problem	$H = 1$	$H = 2$	$H = 3$	$H \geq 4$
1	1	$\in \{T, T \cup R\}$	HSP	$\in P$			
1	> 1	$\in \{T, T \cup R\}$	HMStTP	$\in P$	NP-hard		
> 1	1	T	HMStTP	$\in P$	NP-hard		
> 1	1	$T \cup R$	DMStTP	–	$\in P$	NP-hard	
2	0	R	HSP	$\in P$			
> 2	0	R	DMStTP	–	$\in P$	NP-hard	
≥ 2	≥ 2	$\in \{T, T \cup R\}$	–	–	$\in P$	NP-hard	

2. Generic Formulation

Next we present a generic model for the HSTPMR which will be specialized later on by means of paths and layered graphs.

Let $\mathcal{F} = \{\mathbf{x} \in \{0, 1\}^{|E|} \mid \forall s \in R, \forall t \in T', \exists s - t \text{ path } P \text{ in } E(\mathbf{x}) \text{ s.t. } |P| \leq H\}$ be the set of incidence vectors that contain at least one feasible path between each $s \in R$ and each $t \in T' \setminus \{s\}$, i.e., a path of length at most H . A generic MIP model for the HSTPMR is given by (1)–(7):

$$\min \sum_{\{i,j\} \in E} c_{ij} x_{ij} \tag{1}$$

$$\text{s.t. } x \in \mathcal{F} \tag{2}$$

$$x_{ij} \leq y_i \quad i \in S, \{i, j\} \in E \tag{3}$$

$$\sum_{\{i,j\} \in E} x_{ij} = |R| + |T| + \sum_{i \in S} y_i - 1 \tag{4}$$

$$\sum_{\{i,j\} \in E} x_{ij} \geq 2y_i \quad i \in S \tag{5}$$

$$x_{ij} \in \{0, 1\} \quad \{i, j\} \in E \tag{6}$$

$$y_i \in \{0, 1\} \quad i \in S \tag{7}$$

Constraints (2) ensure that a solution must contain a feasible path for each commodity pair (s, t) . These constraints can be modeled in several ways by using multi-commodity flows, path variables and constraints, or jump inequalities. To discuss the constraints (3)–(5) which, together with (2) ensure that the solution is a tree, we first observe that due to constraints (2) the solution subgraph induced by the hop-constrained paths for all commodities will be connected. Hence, to obtain a valid model, we further add constraints (3) and (4), inequalities (3) to guarantee that a node variable is set to one whenever an incident edge is chosen and equation (4) to ensure that the number of edges in the solution is one less than the number of nodes. Finally, constraints (5) guarantee that the degree of each Steiner node in a feasible solution is at least two, i.e., Steiner nodes cannot be leaves of a solution. Due to the hop constraints these constraints also guarantee that the solution is not disconnected as illustrated by Figure 2. Thus (1)–(7) is a feasible model for the HSTPMR and Figure 2 illustrates that constraints (5) are not redundant in this formulation since omitting them we may obtain isolated components.

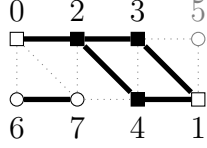


Figure 2: A solution feasible for (1)–(7) without constraints (5) if $T' = T \cup R$ and $H = 3$ that is infeasible for the HSTPMR.

2.1. Disaggregated Path Formulation

In this section, we briefly recall model UPath^{DI} from [14] which turned out to be the best model, both from a theoretical as well as from a computational perspective among all models presented in [14]. Next to already introduced edge and node decision variables, UPath^{DI} used disaggregated arc variables a_{ij}^s , $\forall s \in R$, $\forall (i, j) \in A$, to indicate whether or not arc (i, j) is used when interpreting the solution as an outgoing arborescence rooted at s . Furthermore, the set of all hop constrained paths $\mathcal{W}_{st} \subseteq 2^A$, $|p| \leq H$, $\forall p \in \mathcal{W}_{st}$, from each root $s \in R$ to each relevant terminal $t \in T' \setminus \{s\}$ is considered and an exponential number of path variables $0 \leq \lambda_p^{st} \leq 1$ one for each commodity pair (s, t) , $s \in R$, $t \in T' \setminus \{s\}$, and each feasible path $p \in \mathcal{W}_{st}$ is introduced. Then, a valid path model is obtained by replacing (2) by (8)–(12) in model (1)–(7).

$$a_{ij}^s + a_{ji}^s = x_{ij} \quad s \in R, \{i, j\} \in E \quad (8)$$

$$\sum_{p \in \mathcal{W}_{st}} \lambda_p^{st} = 1 \quad s \in R, t \in T' \setminus \{s\} \quad (9)$$

$$\sum_{p \in \mathcal{W}_{st}: (i, j) \in p} \lambda_p^{st} \leq a_{ij}^s \quad s \in R, t \in T' \setminus \{s\}, (i, j) \in A \quad (10)$$

$$\lambda_p^{st} \geq 0 \quad s \in R, t \in T' \setminus \{s\}, p \in \mathcal{W}_{st} \quad (11)$$

$$a_{ij}^s \in \{0, 1\} \quad s \in R, (i, j) \in A \quad (12)$$

Finally, for UPath^{DI} we add the strengthening constraints (13) and (14) ensuring that the indegree of each node $i \notin R$ is identical for all arborescences and that Steiner nodes cannot be leaves in them. In turn, we remove (4) and (5) since these constraints were shown to be redundant in the resulting model [14].



Figure 3: Layered graphs corresponding to the instance given in Figure 1(a) for $H = 3$ and $T' = T \cup R$. Edges that map back to the solution in Figure 1(b) are drawn in bold.

$$a^s[\delta^-(i)] = \begin{cases} y_i, & i \in S \\ 0, & i = s \\ 1, & \text{else} \end{cases} \quad s \in R, i \in V \quad (13)$$

$$a^s[\delta^+(i)] \geq y_i \quad s \in R, i \in S \quad (14)$$

3. Layered Graph Formulations

Reformulating hop-constrained network design problems using layered graphs recently became a popular technique for obtaining theoretically strong ILP models yielding tight LP bounds. Branch-and-cut algorithms used to solve these models are frequently among the leading approaches for the underlying problems, cf. [13, 17]. In this section we show two different layered graph approaches that can be used to model the HSTPMR.

3.1. Layered Graphs with H Layers

We now introduce one layered graph $G_L^s = (V_L^s, A_L^s)$ for each root node $s \in R$. For every $s \in R$, V_L^s is defined by its root node s_0 , together with nodes i_h , $1 \leq h \leq H - 1$, for all original nodes $i \in V \setminus \{s\}$ and nodes t_H for all other relevant terminals $t \in T' \setminus \{s\}$. For each pair of nodes $i_h, j_{h+1} \in V_L^s$ we add an arc (i_h, j_{h+1}) to A_L^s if $(i, j) \in A$. Formally, for each $s \in R$, $V_L^s = \{s_0\} \cup \{i_h : i \in V \setminus \{s\}, 1 \leq h \leq H - 1\} \cup \{t_H : t \in T' \setminus \{s\}\}$ and $A_L^s = \{(i_h, j_{h+1}) : i_h \in V_L^s, j_{h+1} \in V_L^s, (i, j) \in A\}$; see Figure 3 for an example.

In addition to the previously introduced node and edge design variables, we use two new sets of binary variables to model the problem in the layered graph framework. Variables X_{ij}^{sh} , are associated to arcs $(i_h, j_{h+1}) \in A_L^s$ and are set to one if the corresponding arc is part of the rooted Steiner arborescence in G_L^s , for each $s \in R$. Variables Y_i^{sh} are associated to nodes $i_h \in V_L^s$, $i \in V$, $0 \leq h \leq H$, and are set to one if the corresponding node is part of the rooted Steiner arborescence in G_L^s , for each $s \in R$. The resulting MIP model to which we will refer to as LG is given by (15)–(21) together with (3)–(7).

$$\min \sum_{\{i,j\} \in E} c_{ij} x_{ij} \quad (15)$$

$$\text{s.t. } X^s[\delta^-(i_h)] = Y_i^{sh} \quad s \in R, i_h \in V_L^s, i \neq s \quad (16)$$

$$\sum_{h=1}^H Y_i^{sh} \begin{cases} = 1 & i \in T' \setminus \{s\} \\ \leq 1 & i \in R \setminus (T' \cup \{s\}) \\ \leq y_i & i \in S \end{cases} \quad s \in R, i \in V \quad (17)$$

$$\sum_{(i_{h-1}, j_h) \in A_L^s, i \neq k} X_{ij}^{s, h-1} \geq X_{jk}^{sh} \quad s \in R, (j_h, k_{h+1}) \in A_L^s, j \neq s \quad (18)$$

$$\sum_{h=0}^{H-1} (X_{ij}^{sh} + X_{ji}^{sh}) \leq x_{ij} \quad s \in R, \{i, j\} \in E \quad (19)$$

$$X_{ij}^{sh} \in \{0, 1\} \quad s \in R, (i_h, j_{h+1}) \in A_L^s \quad (20)$$

$$Y_i^{sh} \in \{0, 1\} \quad s \in R, i_h \in V_L^s \quad (21)$$

$$(3) - (7)$$

Indegree constraints (16) link arc to node variables on each layered graph, while constraints (17) ensure that each original node is used at most once on each layered graph and link node variables on the layered graph to original node variables for potential Steiner nodes. Since layered graphs are acyclic, inequalities (18) ensure connectivity on each layered graph, i.e., they guarantee that an arc (j_h, k_{h+1}) emanating from node j_h may only be used if at least one ingoing arc (i_{h-1}, j_h) with $i \neq k$ is selected. Constraints (19) link arc variables on each layered graph to undirected edge variables on the original graph. Figure 4 shows that in the context of this model, that is after adding all the information provided by the layered graph variables, constraints (4) and (5) are still necessary to guarantee that the final solution will be a tree.

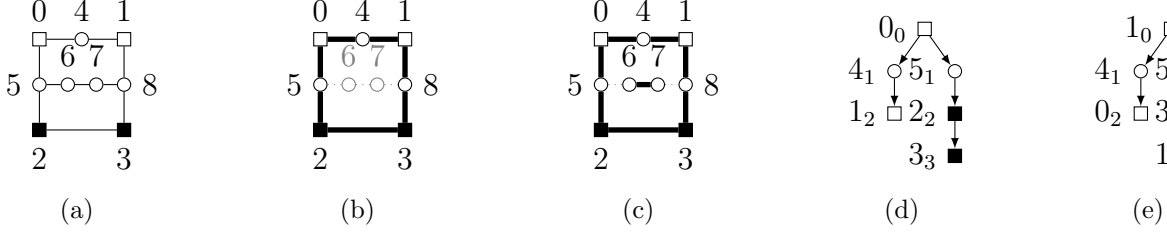


Figure 4: (a) An illustrative instance with $R = \{0, 1\}$ and terminals $T = \{2, 3\}$ that is infeasible for $H = 3$ and $T' = T \cup R$; (b) Solution feasible for LG without (4) and (5); (c) Solution feasible for LG without (5); (d) and (e) Arborescences in G_L^0 and G_L^1 corresponding to (b) and (c).

3.2. Model Enhancements (General)

Acyclicity of each layered graph, allows to eliminate subtours in model LG using a polynomial number of constraints (18). Hence, LG is a compact model which can be solved by LP-based branch-and-bound. It is well known, however, that one can strengthen layered graph based models by adding directed cutset constraints (22) where $V_i^s = \{i_h \in V_L^s \mid 1 \leq h \leq H\}$.

$$X^s[\delta^-(W)] \geq 1, \quad s \in R, \quad t \in T' \setminus \{s\}, \quad W \subseteq V_L^s \setminus \{s_0\}, \quad V_t^s \subseteq W \quad (22)$$

The resulting model will be denoted by LG^C . It contains an exponential number of constraints and can be solved by branch-and-cut (B&C).

3.3. Model Enhancements for $T' = T \cup R$

As pointed out in the introduction, the arborescences for each root share the same set of edges. Thus, we can replace inequalities by equations in (17) and (19), i.e., consider equations (23) and (24) instead.

$$\sum_{h=1}^H Y_i^{sh} = \begin{cases} y_i & i \in S \\ 1 & i \in (R \cup T) \setminus \{s\} \\ 0 & i = s \end{cases} \quad s \in R \quad (23)$$

$$\sum_{h=0}^{H-1} (X_{ij}^{sh} + X_{ji}^{sh}) = x_{ij} \quad s \in R, \quad \{i, j\} \in E \quad (24)$$

We use LG^{CI} to refer to model LG^C where inequalities (17) and (19) are replaced by equations (23) and (24). To make sure that the indegree of each Steiner node does not

exceed its outdegree, we can further add

$$X^s[\delta^+(i_h)] \geq Y_i^{sh} \quad s \in R, i_h \in V_L^s, i \in S \quad (25)$$

to obtain model LG^{CIO} .

Another set of valid inequalities is derived from the fact that the distance between two roots must not depend on the arborescence considered, i.e., on the chosen root. *Root-depth constraints* (26) which are further added to obtain model LG^{CIOR} simply state that if root $q \in R$ is on level h w.r.t. G_L^s , then root $s \in R$ must be on the same level w.r.t. G_L^q .

$$Y_q^{sh} = Y_s^{qh} \quad s \in R, q \in R \setminus \{s\}, 1 \leq h \leq H \quad (26)$$

3.4. The Case $T' = T$: Layered Graphs with $H' = 2H - \text{diam}(T)$ Layers

As pointed out above, the strengthening inequalities (23) and (24) are not valid in this case since we cannot simply ensure that the arborescences for each root share the same set of edges. Corollary 1 permits us to introduce a different layered graph model \hat{G}_L^s containing H' layers for the case $T' = T$ in which all arborescences use the same set of original nodes and edges. In each such graph \hat{G}_L^s the maximum layer $H(i)$ of some original node $i \in V$ is defined as

$$H(i) = \begin{cases} 0 & \text{if } i = s \\ H' & \text{if } i \in R \setminus \{s\} \\ H' - 1 & \text{if } i \in S \\ H & \text{if } i \in T \end{cases}$$

Formally, for each $s \in R$, $\hat{G}_L^s = (\hat{V}_L^s, \hat{A}_L^s)$ is defined by $\hat{V}_L^s = \{s_0\} \cup \{i_h : i \in V \setminus \{s\}, 1 \leq h \leq H(i)\}$ and $\hat{A}_L^s = \{(i_h, j_{h+1}) : i_h \in \hat{V}_L^s, j_{h+1} \in \hat{V}_L^s, (i, j) \in A\}$.

Based on this observations, model (27)–(33) to which we will refer to as LG_E uses the same set of variables as the previous model. Note, however, that for this case we consider H' layers which is almost as twice as the number of layers in the original graph. On the other hand, the model defined in this extended layered graph permits us to use the strengthening inequalities that have been used for the $T' = T \cup R$ case.

$$\min \sum_{\{i,j\} \in E} c_{ij} x_{ij} \quad (27)$$

$$\text{s.t. } X^s[\delta^-(i_h)] = Y_i^{sh} \quad s \in R, i_h \in \hat{V}_L^s, i \neq s \quad (28)$$

$$\sum_{h=1}^{H(i)} Y_i^{sh} = \begin{cases} 1 & i \in (T \cup R) \setminus \{s\} \\ y_i & i \in S \end{cases} \quad s \in R, i \in V \quad (29)$$

$$\sum_{(i_{h-1}, j_h) \in \hat{A}_L^s, i \neq k} X_{ij}^{s,h-1} \geq X_{jk}^{sh} \quad s \in R, (j_h, k_{h+1}) \in \hat{A}_L^s, j \neq s \quad (30)$$

$$\sum_{h=0}^{H(i)} X_{ij}^{sh} + \sum_{h=0}^{H(j)} X_{ji}^{sh} = x_{ij} \quad s \in R, \{i, j\} \in E \quad (31)$$

$$X_{ij}^{sh} \geq 0 \quad s \in R, (i_h, j_{h+1}) \in \hat{A}_L^s \quad (32)$$

$$Y_i^{sh} \geq 0 \quad s \in R, i_h \in \hat{V}_L^s \quad (33)$$

$$(5) - (7)$$

Note that, we do not include constraints (3) and (4) in model LG_E since they are redundant as we will prove in Section 4. As previously discussed, by considering directed cutset constraints (34) we can obtain a stronger model LG_E^{C} which contains an exponential number of constraints. To avoid that Steiner nodes may be leaves in any of the arborescences, we further add inequalities (35) yielding model LG_E^{CO} . Finally, by the same arguments as before root-depth constraints (36) are valid and we will use LG_E^{COR} to refer to the resulting model.

$$X^s[\delta^-(W)] \geq 1 \quad s \in R, t \in (T \cup R) \setminus \{s\}, W \subseteq \hat{V}_L^s \setminus \{s_0\}, \\ \{t_h : 1 \leq h \leq H(t)\} \subseteq W \quad (34)$$

$$X^s[\delta^+(i_h)] \geq Y_i^{sh} \quad s \in R, i_h \in \hat{V}_L^s, i \in S \quad (35)$$

$$Y_q^{sh} = Y_s^{qh} \quad s \in R, q \in R \setminus \{s\}, 1 \leq h \leq H' \quad (36)$$

4. Polyhedral Comparison

In this section we compare the different formulations with respect to the value of their LP relaxation. In Section 4.1 we address the case $T' = T \cup R$ and in Section 4.2 we address that case $T' = T$. We also show that some set of constraints become redundant after the addition of some sets of valid inequalities.

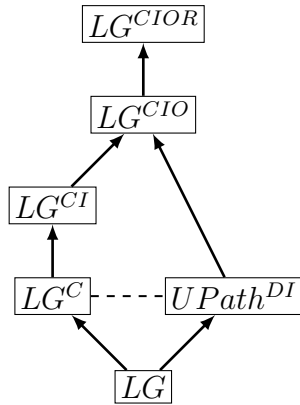
By \mathcal{P}_M we will denote the convex hull of all feasible LP solutions of a MIP formulation M and by $\text{proj}_{\mathbf{a}^1, \dots, \mathbf{a}^n}(\mathcal{P}_M)$, the orthogonal projection of the convex hull of LP solutions of M onto the space defined by variables $\mathbf{a}^1, \dots, \mathbf{a}^n$. Furthermore, by $v_{\text{LP}}(\cdot)$ we denote the value of the LP relaxation of some model. When comparing two formulations F_1 and F_2 , we say F_1 is stronger than F_2 if $v_{\text{LP}}(F_2) \leq v_{\text{LP}}(F_1)$ and strictly stronger if there additionally exist instances for which strict inequality holds. Furthermore, if for two formulations, none of them is stronger than the other, we say that they are incomparable. In many cases strict dominance follows due to the computational results that will be discussed in Section 5.1. Usually, however, we will additionally provide solutions that are feasible for one model and not feasible for the other. In some cases these figures will be left for the Appendix.

For better readability, Table 2 provides a summary of all model variants and their definitions.

4.1. Polyhedral comparison for $T' = T \cup R$

The following theorem which is proved by a series of subsequent lemmas summarizes the obtained relations between the considered models when $T' = T \cup R$.

Theorem 4.1. *For $T' = T \cup R$, the following relations hold:*



Thereby, an arrow indicates that the formulation at the target is strictly stronger than the one at the source while a dashed edge indicates that the corresponding formulations are incomparable.

Lemma 3. *Formulation LG^{C} is strictly stronger than formulation LG .*

We skip the proof of this lemma, since it is well known that the result holds for the case of a single root and the result easily extends to multiple roots.

Lemma 4. *Formulation LG^{CI} is strictly stronger than formulation LG^{C} . Furthermore, constraints (3) and (4) are redundant in LG^{CI} .*

Table 2: Overview on the considered models.

Model	T'	Definition
UPath ^{DI}	$\in \{T, T \cup R\}$	(1), (3), (6), (7), (8)–(14)
LG	$\in \{T, T \cup R\}$	(15)–(21), (3)–(7)
LG ^C	$\in \{T, T \cup R\}$	LG, (22)
LG ^{CI}	$T \cup R$	LG ^C , (23), (24)
LG ^{CIO}	$T \cup R$	LG ^{CI} , (25)
LG ^{CIOR}	$T \cup R$	LG ^{CIO} , (26)
LG _E	T	(27)–(33), (5)–(7)
LG _E ^C	T	LG _E , (34)
LG _E ^{CO}	T	LG _E ^C , (35)
LG _E ^{COR}	T	LG _E ^{CO} , (36)

Proof. Since LG^{CI} contains all constraints of model LG^C it is sufficient to consider the example given in Figure 8 in the Appendix which shows that constraints (23) and (19) improve the LP bound. Computational results given in Section 5.1 further show this relation.

To prove the second result, consider an arbitrary root $s \in R$ and edge $\{i, j\} \in E$ incident to some potential Steiner node $i \in S$. To see that constraints (3) are redundant we use equations (24), (18), (16), and (23) together with the fact that the minimum and maximum layer of nodes i_h corresponding to potential Steiner nodes i is 1 and $H - 1$, respectively:

$$\begin{aligned}
 x_{ij} &\stackrel{(24)}{=} \sum_{h=0}^{H-1} (X_{ji}^{sh} + X_{ij}^{sh}) = \sum_{h=0}^{H-2} X_{ji}^{sh} + \sum_{h=1}^{H-1} X_{ij}^{sh} \stackrel{(18)}{\leq} \\
 &\leq \sum_{h=0}^{H-2} X_{ji}^{sh} + \sum_{h=0}^{H-2} \sum_{\substack{(k_h, i_{h+1}) \in A_L^s, \\ k \neq j}} X_{ki}^{sh} = \sum_{h=1}^{H-1} X^s[\delta^-(i_h)] \stackrel{(16)}{=} \sum_{h=1}^{H-1} Y_i^{sh} \stackrel{(23)}{=} y_i
 \end{aligned}$$

To show that equation (4) is implied:

$$\begin{aligned}
 \sum_{\{i,j\} \in E} x_{ij} &\stackrel{(24)}{=} \sum_{\{i,j\} \in E} \sum_{h=0}^{H-1} (X_{ij}^{sh} + X_{ji}^{sh}) = \sum_{i \in V} \sum_{h=1}^H X^s[\delta^-(i_h)] \stackrel{(16)}{=} \\
 &\stackrel{(16)}{=} \sum_{i \in V} \sum_{h=1}^H Y_i^{sh} \stackrel{(23)}{=} |R| + |T| + \sum_{i \in S} y_i - 1
 \end{aligned}$$

□

Lemma 5. *Formulation LG^{CIO} is strictly stronger than formulation LG^{CI}. Furthermore, inequalities (5) are redundant in LG^{CIO}.*

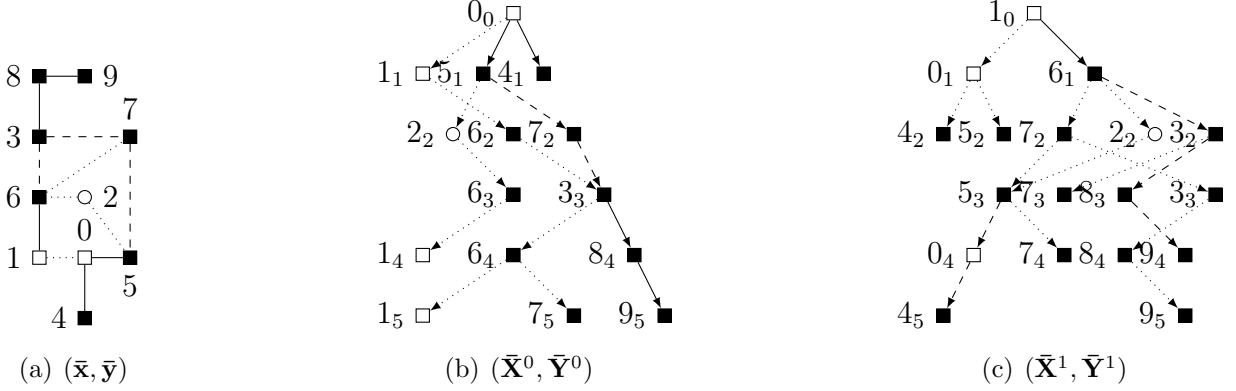


Figure 5: A feasible solution $(\bar{x}, \bar{y}, \bar{X}, \bar{Y})$ to the LP relaxation of LG^{CI} of an instance with $R = \{0, 1\}$, $T = \{3, 4, 5, 6, 7, 8, 9\}$, $H = 5$, and $T' = T \cup R$. (a) Subgraph induced by variable values \bar{x}_e , $e \in E$; $\bar{y}_3 = 1/3$. (b), (c) Subgraphs induced by variable values \bar{X}_{ij}^{sh} , $s \in \{0, 1\}$, $(i_h, j_{h+1}) \in A_L^s$, respectively. Solid edges and arcs indicate a variable value of 1, dashed edges and arcs of $2/3$ and dotted edges and arcs of $1/3$.

Proof. Since LG^{CIO} contains all constraints of LG^{CI} , it only remains to show that LG^{CIO} is strictly stronger. This relation can be seen from the computational results discussed in Section 5.1. In addition, Figure 9 in the Appendix illustrates an example that is feasible for the LG^{CI} model, but it violates inequalities (25).

Finally, for each potential Steiner nodes $i \in S$, inequalities (5) are redundant since:

$$\begin{aligned}
\sum_{\{i,j\} \in \delta(i)} x_{ij} &\stackrel{(24)}{=} \sum_{\{i,j\} \in \delta(i)} \sum_{h=0}^{H-1} (X_{ij}^{sh} + X_{ji}^{sh}) = \sum_{h=1}^H X^s[\delta^-(i_h)] + \sum_{h=0}^{H-1} X^s[\delta^+(i_h)] \\
&\stackrel{(16),(25)}{\geq} \sum_{h=1}^H Y_i^{sh} + \sum_{h=0}^{H-1} Y_i^{sh} \stackrel{(24)}{=} 2y_i
\end{aligned}$$

□

Lemma 6. *Formulation LG^{CIOR} is strictly stronger than formulation LG^{CIO} .*

Proof. Since LG^{CIOR} contains all constraints of LG^{CIO} , it only remains to show that root-depth constraints (26) can be violated in an optimal LP solutions of model LG^{CIO} . Consider the solution shown in Figure 5 feasible for LG^{CIO} ($H = 5$; $T' = T \cup R$). Clearly, inequalities (26) are violated since $\tilde{Y}_1^{05} \neq \tilde{Y}_0^{15}$ and also $\tilde{Y}_1^{04} \neq \tilde{Y}_0^{14}$.

It remains to show that, for solution values (\bar{x}, \bar{y}) corresponding to Figure 5(a) we cannot find a different set of feasible vectors $(\tilde{X}^s, \tilde{Y}^s)$, $s \in \{0, 1\}$, that satisfy constraints (26). This is established by the following two observations which will be proved in the following:

1. For any solution vector $(\tilde{\mathbf{X}}^0, \tilde{\mathbf{Y}}^0)$ feasible w.r.t. $(\bar{\mathbf{x}}, \bar{\mathbf{y}})$, $\tilde{Y}_1^{05} \geq 1/3$ holds.
2. For any solution vector $(\tilde{\mathbf{X}}^1, \tilde{\mathbf{Y}}^1)$ feasible w.r.t. $(\bar{\mathbf{x}}, \bar{\mathbf{y}})$, $\tilde{Y}_0^{15} = 0$ holds.

To see that $\tilde{Y}_1^{05} = 1/3$ must hold, note that each path in 5(a) between nodes 0 and 3 consists of at least three edges. Since $H = 5$ and we need to establish a feasible connection from 0 to 9, this implies that $\tilde{Y}_3^{03} = 1$ and thus through the path 0-5-7-3 and 0-1-6-3 we send $2/3$ and $1/3$ units of flow, respectively. Since indegree of 6 and 7 needs to be one, $1/3$ units of flow are sent through $(6, 7)$, $(3, 6)$, $(2, 6)$. Consequently, $1/3$ units of flow has to be sent along 0-5-7-3-6-1 to reach node 1 which means that $\tilde{Y}_1^{05} \geq 1/3$.

Note that $\tilde{Y}_0^{15} = 0$ means that node 0 cannot be at the last layer. To see that this holds observe that terminal 4 can only be reached through node 0. Therefore, when 1 is taken as the root, the maximal layer for node 0 is four. \square

Lemma 7. *Formulation UPath^{DI} is strictly stronger than formulation LG.*

Proof. Let $(\bar{\mathbf{x}}, \bar{\mathbf{y}}, \bar{\mathbf{a}}, \bar{\boldsymbol{\lambda}})$ be an optimal solution to the LP relaxation of formulation UPath^{DI}. We first show how to derive a solution $(\bar{\mathbf{x}}, \bar{\mathbf{y}}, \bar{\mathbf{X}}, \bar{\mathbf{Y}}) \in \mathcal{P}_{\text{LG}}$ with the same objective value. The main difficulty in this derivation is that the linking constraints (19) of model LG sum over all copies of one edge $e \in E$ while the linking constraints (8) of model UPath^{DI} consider each terminal individually. Thus, for each $s \in R$ and each arc $(i, j) \in A$, we use values of the variables \bar{a}_{ij}^s to obtain the values of the variables $\bar{X}_{ij}^{sh}, (i_h, j_{h+1}) \in A_L^s, 0 \leq h \leq H - 1$ as follows:

$$\bar{X}_{ij}^{sh} = \begin{cases} \bar{a}_{ij}^s & \text{if } i = s \\ \max\{0, \min\{\bar{a}_{ij}^s, \sum_{(k_{h-1}, i_h) \in A_L^s: k \neq j} \bar{X}_{ki}^{s, h-1}\} - \sum_{h'=0}^{h-1} \bar{X}_{ij}^{sh'}\} & \text{otherwise} \end{cases} \quad (37)$$

For each root s and for each arc (i, j) , the values \bar{X}_{ij}^{sh} are defined recursively w.r.t. the layers starting from the root. Available capacities \bar{a}_{ij}^s are distributed among the layers while respecting the connectivity constraints (18) and ensuring that $\sum_{h=0}^{H-1} \bar{X}_{ij}^{sh} \leq \bar{a}_{ij}^s$. We note that since $\bar{a}^s[\delta^-(i)] \leq 1, \forall i \in V$, cf. (13), we can use equations (16) to set variable values $\bar{Y}_i^{sh}, \forall s \in R, \forall i_h \in V_L^s$. To see that inequalities (17) hold, we first observe that for each node $i \in V$, we have

$$\sum_{h=1}^H \bar{Y}_i^{sh} \stackrel{(16)}{=} \sum_{h=1}^H \bar{X}^s[\delta^-(i_h)] = \sum_{(j,i) \in A} \sum_{h=1}^H \bar{X}_{ji}^{sh} \stackrel{(37)}{\leq} \sum_{(j,i) \in A} \bar{a}_{ji}^s \stackrel{(13)}{=} \begin{cases} \bar{y}_i & i \in S \\ 0 & i = s \\ 1 & \text{else} \end{cases}$$

It remains to prove that for each root $s \in R$ and each terminal $t \in T' \setminus \{s\}$, $\sum_{h=1}^H \bar{Y}_t^{sh} = 1$ does hold. First observe that due to (9), (10), and (13) for each arc (u, t) we have $\sum_{p \in \mathcal{W}_{st}: (u,t) \in p} \bar{\lambda}_p^{st} = \bar{a}_{ut}^s$. Furthermore, for each arc (i, j) , $i \neq s$, contained in the used set of paths from s to t , i.e., in the set $\{p \in \mathcal{W}_{st} \mid \bar{\lambda}_p > 0\}$, we have $\sum_{p \in \mathcal{W}_{st} | (i,j) \in p} \bar{\lambda}_p \leq \sum_{p \in \mathcal{W}_{st} | (k,i) \in p, k \neq j} \bar{\lambda}_p$ since flow balance holds for each path. Thus, due to (37) we will distribute the total available capacity \bar{a}_{it}^s for each arc (i, t) with $t \in T' \setminus \{s\}$ on the arcs of the layered arborescence with root s , i.e., $\sum_{h=1}^H \bar{X}^s[\delta^-(t_h)] = \sum_{h=1}^H \bar{Y}_t^{sh} = \bar{a}^s[\delta^-(t)] = 1$.

To see that the inequality can be strict consider the LP-solution $(\bar{\mathbf{x}}, \bar{\mathbf{y}}, \bar{\mathbf{X}}, \bar{\mathbf{Y}})$ given in Figure 8 (see Appendix) feasible for LG. It is, however, not possible to derive assignments of variable values \mathbf{a}^0 and \mathbf{a}^1 that satisfy all constraints of model UPath^{DI}. \square

Lemma 8. *Formulations UPath^{DI} and LG^C are incomparable.*

Proof. We first consider the solution given in Figure 8 which is a feasible LP-solution of LG^C but infeasible for the LP relaxation of UPath^{DI}. Hence, it suffices to additionally consider an LP-solution feasible for UPath^{DI} which is infeasible for LG^C. As already observed by Gouveia et al. [13] for the single root case a path formulation allows to use the full capacity of arcs at different positions in paths to different terminals, while in a layered graph formulation total capacity must be equal to the sum of capacities on different positions independently of the considered terminal. Their example can be generalized to the multiple root case in a straightforward way. \square

Lemma 9. *Formulation LG^{CIO} is strictly stronger than formulation UPath^{DI}.*

Proof. We show that given an LP solution $(\bar{\mathbf{x}}, \bar{\mathbf{y}}, \bar{\mathbf{X}}, \bar{\mathbf{Y}})$ of LG^{CIO} we can construct a solution $(\bar{\mathbf{x}}, \bar{\mathbf{y}}, \bar{\mathbf{a}}, \bar{\boldsymbol{\lambda}}) \in \mathcal{P}_{\text{UPath}^{\text{DI}}}$ using

$$\bar{a}_{ij}^s := \sum_{h=0}^{H-1} \bar{X}_{ij}^{sh} \quad \forall s \in R, \forall (i, j) \in A \quad (38)$$

Hereby, to simplify the notation we assume that $\bar{X}_{ij}^{sh} = 0$ if $(i_h, j_{h+1}) \notin A_L^s$. From Lemma 4 we conclude that inequalities (3) are satisfied since they are implied by model LG^{CIO}. Constraints (8) follow due to (38) and (24). Furthermore, from the directed cutset constraints (22), using the max-flow min-cut theorem together with the path decomposition of the flow we can construct the necessary set of paths on the layered graph for each root $s \in R$ and each relevant terminal $t \in T' \setminus \{s\}$. Since hop constraints are implicitly satisfied in the structure of the layered graph, constraints (9) and (10) are satisfied. Using (38), (16),

and (23) we show that equations (13) are satisfied as follows:

$$\sum_{(j,i) \in A} \bar{a}_{ji}^s \stackrel{(38)}{=} \sum_{(j,i) \in A} \sum_{h=0}^{H-1} \bar{X}_{ji}^{sh} = \sum_{h=1}^H \bar{X}^s[\delta^-(i_h)] \stackrel{(16)}{=} \sum_{h=1}^H \bar{Y}_i^{sh} \stackrel{(23)}{=} \begin{cases} \bar{y}_i & i \in S \\ 0 & i = s \\ 1 & \text{else} \end{cases}$$

Finally, using the fact that potential Steiner nodes $i \in S$ do not exist in any layered graph at layer H , inequalities (14) hold for each root $s \in R$ since

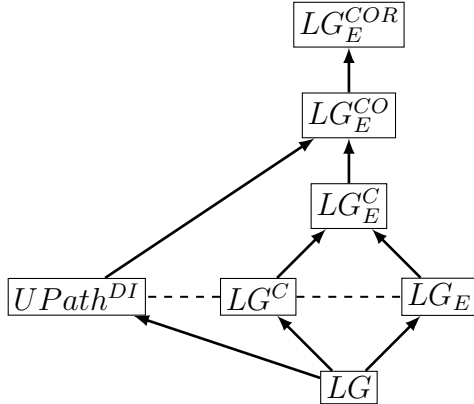
$$\sum_{(i,j) \in A} \bar{a}_{ij}^s \stackrel{(38)}{=} \sum_{(i,j) \in A} \sum_{h=0}^{H-1} \bar{X}_{ij}^{sh} = \sum_{h=0}^{H-1} \bar{X}^s[\delta^+(i_h)] \stackrel{(25)}{\geq} \sum_{h=0}^{H-1} \bar{Y}_i^{sh} \stackrel{(23)}{=} \bar{y}_i.$$

To see that the inclusion can be strict, we refer again to the previously mentioned straightforward generalization of the example provided by Gouveia et al. [13] for the single root case. \square

4.2. Polyhedral comparison for $T' = T$

In this subsection we prove similar results for the case $T' = T$. Again, the following theorem is proved by a series of subsequent lemmas.

Theorem 4.2. *For $T' = T$, the following relations hold:*



Thereby, an arrow indicates that the formulation at the target is strictly stronger than the one at the source while a dashed edge indicates that the corresponding formulations are incomparable.

In what follows, we will prove only those results stated in the latter theorem that are non-trivial and cannot be derived in a similar way as for the case $T' = T \cup R$.

Lemma 10. *Formulation LG^C is strictly stronger than formulation LG . Furthermore, formulation LG_E^C is strictly stronger than formulation LG_E .*

We skip the proof of this result since it is well known for the case of one root and it is easy to find examples showing that the directed cutset constraints can be violated in optimal LP solutions of models LG and LG_E , respectively.

Lemma 11. *Formulation LG_E is strictly stronger than formulation LG and formulation LG_E^C is strictly stronger than formulation LG^C . Furthermore, constraints (3) and (4) are redundant in LG_E .*

Proof. To see that LG_E is stronger than LG, we observe that it essentially differs from model LG by equations (29) which are lifted variants of inequalities (17) and equations (31) which are stronger versions of inequalities (19). To see that the relation is strict, we consider the LP-solution of LG corresponding to Figure 6 and note that we cannot find a layered arborescence with root 1 feasible for LG_E , i.e., such that the indegree of node 0 is one, without increasing the variable value x_{01} or x_{03} .

The same arguments can be used when considering the formulations with directed cutset constraints, i.e., LG_E^C and LG^C . Redundancy of constraints (3) and (4) in LG_E can be shown using an analogous deduction as in Lemma 4 for the case $T' = T \cup R$. \square

Lemma 12. *Formulations LG_E and LG^C are incomparable.*

Proof. We first observe that if $T' = T$, the solution given in Figure 6 is a valid LP solution for LG^C . As argued before, however, we cannot find a feasible arborescence with root 1 such that the indegree of 0 (and all terminals) is one. Since this argument does not depend on the maximum allowed path length (and thus on the number of layers on a layered graph) this solution is infeasible for LG_E . On the other hand, it is well known that the directed cutset constraints (22) can be violated in optimal LP-solutions of LG_E . \square

Lemma 13. *Formulation LG_E^{CO} is strictly stronger than formulation LG_E^C . Formulation LG_E^{COR} is strictly stronger than formulation LG_E^{CO} . Furthermore, constraints (5) are redundant in LG_E^{CO} .*

Proof. LG_E^{COR} contains all constraints of LG_E^{CO} which in turn contains all constraints of LG_E^C . Strict inequality can be seen by modifying the previously discussed exemplary solutions given in Figures 5 and 9 to the case $T' = T$. Redundancy of inequalities (5) in LG_E^{CO} can be shown in an analogous way as for the case $T' = T \cup R$ in Lemma 5. \square

Lemma 14. *Formulation UPath^{DI} is strictly stronger than formulation LG. Furthermore, formulation LG_E^{CO} is strictly stronger than formulation UPath^{DI} .*

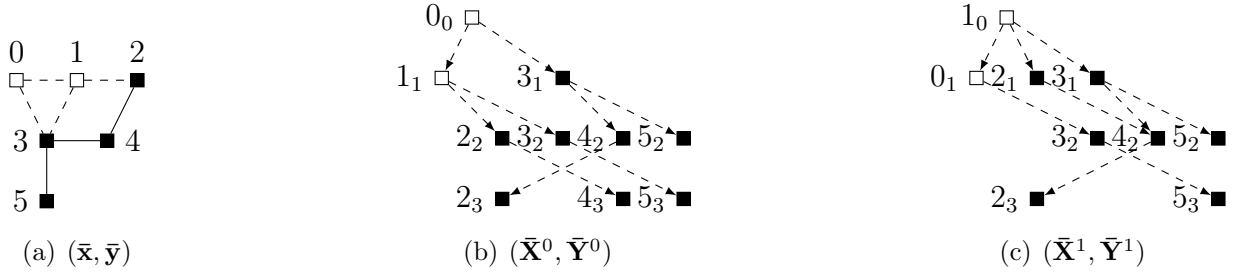


Figure 6: A feasible solution $(\bar{x}, \bar{y}, \bar{X}, \bar{Y})$ to the LP relaxation of LG or LG^C of an instance with $R = \{0, 1\}$, $T = \{2, 3, 4, 5\}$, $T' = T$, and $H = 3$. (a) Subgraph induced by variable values \bar{x}_e , $e \in E$. (b), (c) Subgraphs induced by variable values $\bar{X}_{ij}^{s_h}$, $s \in \{0, 1\}$, $(i_h, j_{h+1}) \in A_1^s$, respectively. Solid edges indicate a corresponding variable value of 1 while dashed edges and arcs indicate a variable value of $1/2$.

Proof. One can prove that UPath^{DI} is stronger than LG and that LG_E^{CO} is stronger than UPath^{DI} using analogous arguments than for the case $T' = T \cup R$, cf., Lemmas 7 and 9. To see that the first relation can be strict consider the previously discussed example given in Figure 6 which provides a feasible LP solution of LG which is infeasible for UPath^{DI} . For the second relation, again consider the previously mentioned straightforward generalization of the example from [13] to the case with more than one root node. \square

Lemma 15. *Formulations LG^C and UPath^{DI} are incomparable.*

Proof. As mentioned before for the case $T' = T \cup R$ an exemplary LP-solution feasible for UPath^{DI} but infeasible for LG^C can be constructed as a straightforward generalization from the single root case [13]. On the other hand, as discussed in Lemma 12 the solution given in Figure 6 is feasible for LG^C but we cannot find a feasible orientation with root 1 such that the indegree of 0 is one, i.e., the solution is infeasible for the LP-relaxation of UPath^{DI} . \square

5. Computational Study

In this section, we detail all components of the implemented branch-and-cut algorithms (B&C) for the different variants of LG and LG_E and of the column generation approach (CG) used to solve the LP relaxation of UPath^{DI} . All approaches are implemented in C++ using IBM CPLEX 12.4 and all experiments have been performed on a single core of an Intel Xeon processor with 2.53 GHz using at most 3GB RAM.

For the separation of directed cutset constraints (22) or (34), respectively, we run the maximum flow algorithm of Cherkassky and Goldberg [2]. In all separation variants, we use nested and backcuts, cf. [18], and insert at most 100 violated cuts in each iteration. If

a particular model considers outdegree constraints on potential Steiner nodes, cf. (25) and (35), or root-depth inequalities, cf. (26) or (36), they are separated dynamically, rather than statically inserted in the beginning, since preliminary tests showed that typically only very few of them will be violated.

In the column generation approach of UPath^{DI}, a hop constrained shortest path problem between each root and each relevant node on a graph with nonnegative arc costs needs to be solved in order to solve the pricing subproblem. As originally proposed by Gouveia et al. [11] for a spanning tree problem with distance constraints we potentially add multiple path variables for each root terminal pair by considering the shortest paths to all nodes adjacent to a currently considered relevant node for all hop values $0 \leq h \leq H - 1$, for more details see [14].

Benchmark Instances. Evaluation and comparison of the approaches and models is conducted on benchmark instances from [13] that are typically used for testing HMSTP and DMSTP approaches. We chose the first instance from each of the groups of random (R) and Euclidean instances (C) with 31, 41, and 61 nodes. For the sake of simplicity we will use 30, 40, and 60 to refer to them. All graphs are complete and we use the first $|T|$ nodes as terminals and the last $|R|$ nodes as roots. In our experiments, we choose $|R| \in \{2, 4, 6, 8\}$, $|T| \in \{5, 10, 15, 20\}$, and test all possible combinations for hop limits $H = 3, \dots, 6$ and $T' \in \{T, T \cup R\}$.

5.1. Computational Results

Tables 3 and 4 detail our results regarding the LP relaxations of all proposed models for $T' = T \cup R$ and $T' = T$, respectively. Results are grouped by instance sets, numbers of root nodes, and the hop limit. The tables provide information on: the total number of instances in each group ($\#$), the number of instances for which the LP relaxation of a particular model could be solved within 7,200 CPU-seconds ($\#_{\text{solved}}$), geometric means of the corresponding CPU-times, the numbers of instances for which the LP relaxation is integral ($\#_{\text{int}}$), average and maximum LP gaps in percent calculated by $(\text{OPT} - v_{\text{LP}}(\cdot))/\text{OPT}$. Notice, that $\#_{\text{all}}$ denotes the number of instances for which the LP-relaxation could be solved by all models and for which the optimal IP solution is known. The values for $\#_{\text{int}}$, average and maximum gaps are calculated only among those instances.

We first observe that solving the LP relaxation of UPath^{DI} needs significantly more CPU-time than solving the LP-relaxation of any of the layered graph models both for $T' = T \cup R$ and for $T' = T$. Furthermore, model UPath^{DI} is not only theoretically dominated by the

Table 3: Results for solving LP relaxations in case $T' = T \cup R$ grouped by instance set, $|R|$, and H . Numbers of solved instances ($\#_{\text{solved}}$), geometric means of CPU-times in seconds, numbers of instances solved by all approaches and where IP optimum is known ($\#_{\text{all}}$), numbers of instances where LP relaxation is integral ($\#_{\text{int}}$), average and maximum LP relaxation gaps in %. P and L are used as abbreviations for UPath^{DI} and LG, respectively; time limit: 7 200 CPU-seconds.

	#	#solved					CPU-time [s]						#all	#int						Avg. Gap [%]						Max. Gap [%]							
		P	L	L ^C	L ^{CI}	L ^{CIO}	L ^{CIOR}	P	L	L ^C	L ^{CI}	L ^{CIO}		L ^{CIOR}	P	L	L ^C	L ^{CI}	L ^{CIO}	L ^{CIOR}	P	L	L ^C	L ^{CI}	L ^{CIO}	L ^{CIOR}	P	L	L ^C	L ^{CI}	L ^{CIO}	L ^{CIOR}	
Set	C30 64	33	64	61	60	60	59	826	18	59	49	49	55	33	25	4	27	27	27	27	27	0.6	5.8	0.4	0.4	0.4	0.3	6.3	14.9	4.2	4.2	4.2	4.2
	C40 64	23	64	51	52	52	48	2324	80	374	296	298	333	23	18	1	20	20	20	20	0.4	8.9	0.2	0.2	0.2	0.2	4.8	15.5	2.3	2.3	2.3	2.3	
	C60 64	14	54	38	37	35	36	4704	465	1559	1579	1613	1608	13	8	0	8	8	8	8	0.9	10.6	0.7	0.7	0.7	0.7	3.6	17.9	3.3	3.3	3.3	3.3	
	R30 64	38	64	64	64	64	64	1014	9	15	12	13	16	38	20	17	19	23	24	24	2.2	4.1	2.5	1.7	1.6	1.5	10.4	14.0	12.8	8.7	8.7	8.6	
	R40 64	25	64	59	59	58	57	2277	54	166	178	197	234	24	12	3	13	14	14	15	3.6	8.6	4.3	2.2	2.2	2.1	19.9	29.3	22.5	11.8	11.8	11.5	
	R60 64	15	59	50	46	45	43	4438	249	473	621	652	744	15	3	2	3	5	5	6	8.3	13.1	10.7	4.3	4.0	3.6	25.2	30.8	28.5	14.3	13.9	13.8	
R	2 96	86	96	96	96	96	96	183	4	9	8	8	8	86	55	13	58	61	62	63	1.5	7.5	1.8	1.0	1.0	0.9	25.2	30.0	25.7	14.3	13.9	13.8	
	4 96	46	96	93	93	92	92	2719	46	115	108	121	136	44	22	8	24	26	26	27	3.7	7.9	4.3	2.2	2.1	2.0	20.7	30.8	28.5	8.7	8.7	8.6	
	6 96	13	93	77	73	72	68	5835	193	601	592	605	705	13	8	5	7	9	9	9	2.5	5.8	2.7	1.4	1.4	1.2	19.9	29.3	22.5	11.8	11.8	11.5	
	8 96	3	84	57	56	54	51	7066	556	1949	2002	2034	2352	3	1	1	1	1	1	1	4.0	8.4	3.2	2.0	2.0	1.9	6.3	13.1	6.4	3.1	3.1	2.9	
H	3 96	51	96	94	94	94	92	1134	18	51	55	58	68	51	15	0	16	21	21	23	3.9	9.2	4.7	2.1	2.1	1.9	20.7	30.8	28.5	11.8	11.8	11.5	
	4 96	38	96	86	83	81	78	2145	52	168	184	198	228	37	23	7	25	25	26	3.1	8.5	3.4	2.2	2.0	1.9	25.2	30.0	25.7	14.3	13.9	13.8		
	5 96	31	92	75	74	73	71	2717	105	330	300	317	367	31	23	7	23	25	25	25	0.6	5.8	0.7	0.6	0.6	0.5	8.6	17.0	10.6	8.6	8.5	8.1	
	6 96	28	85	68	67	66	66	3097	182	421	316	325	327	27	25	13	26	26	26	26	0.1	4.7	0.0	0.0	0.0	0.0	0.7	17.9	0.3	0.3	0.3	0.3	

23

Table 4: Results for solving LP relaxations in case $T' = T$ grouped by instance set, $|R|$, and H . Numbers of solved instances ($\#_{\text{solved}}$), geometric means of CPU-times in seconds, numbers of instances solved by all approaches and where IP optimum is known ($\#_{\text{all}}$), numbers of instances where LP relaxation is integral ($\#_{\text{int}}$), average and maximum LP-gaps in %. P and L are used as abbreviations for UPath^{DI} and LG, respectively; time limit: 7 200 CPU-seconds.

	#	#solved						CPU-time [s]						#all	#int						Avg. Gap [%]						Max. Gap [%]										
		P	L	L ^C	L _E ^C	L _E ^{CO}	L _E ^{COR}	P	L	L ^C	L _E ^C	L _E ^{CO}	L _E ^{COR}		P	L	L ^C	L _E ^C	L _E ^{CO}	L _E ^{COR}	P	L	L ^C	L _E ^C	L _E ^{CO}	L _E ^{COR}	P	L	L ^C	L _E ^C	L _E ^{CO}	L _E ^{COR}					
Set	C30 64	40	64	57	64	57	56	600	16	116	21	93	114	121	40	29	0	27	4	32	32	33	0.6	11.5	0.7	5.8	0.4	0.4	0.3	5.0	21.1	6.8	14.9	4.2	4.2	4.2	
	C40 64	28	64	46	62	44	45	40	2031	61	487	132	552	620	703	26	19	0	20	2	21	21	23	0.6	13.9	0.6	8.3	0.3	0.3	0.2	5.5	26.1	6.9	15.5	3.2	3.2	2.5
	C60 64	16	60	31	42	28	29	26	4413	364	2082	853	2657	2672	2747	13	8	0	7	0	8	8	8	0.9	15.2	0.9	9.8	0.7	0.7	0.7	3.6	25.4	3.3	17.9	3.3	3.3	3.3
	R30 64	48	64	64	64	64	64	63	754	10	19	14	26	31	36	48	22	16	21	19	22	26	27	2.8	5.7	3.2	4.6	2.6	2.4	2.2	11.1	25.8	13.4	18.6	10.1	9.6	9.4
	R40 64	31	64	57	62	51	48	48	1904	42	176	109	350	425	487	26	12	2	11	3	12	12	12	3.8	10.8	4.8	8.0	3.3	3.0	2.9	16.8	35.2	21.1	28.9	14.8	14.0	13.8
	R60 64	16	61	45	49	39	35	33	3992	191	532	502	994	1432	1540	15	3	2	3	2	3	4	4	9.2	14.1	11.0	12.1	8.3	5.7	5.4	25.7	35.2	29.9	30.0	24.8	16.9	16.8
R	2 96	86	96	96	96	96	96	188	4	11	4	13	15	16	86	55	11	57	13	58	61	61	1.6	8.5	1.8	7.3	1.4	1.0	1.0	25.2	30.0	25.7	30.0	24.8	14.1	13.9	
	4 96	52	96	91	93	87	85	83	2027	39	160	85	242	306	359	49	22	5	22	9	23	24	24	4.2	13.2	4.8	7.5	3.6	3.2	3.0	25.7	35.2	29.9	28.9	20.8	16.9	16.8
	6 96	28	96	68	84	59	60	56	4399	145	855	409	1227	1435	1592	22	10	4	8	6	10	11	15	2.5	11.7	3.1	5.6	2.1	2.0	1.8	11.3	26.1	14.9	18.2	11.1	11.0	10.7
	8 96	13	89	45	70	41	37	31	5870	394	2446	1070	3088	3421	3765	11	6	0	2	2	7	7	7	2.3	13.7	3.5	6.3	2.0	2.0	1.8	8.5	25.8	10.4	18.6	8.3	8.2	7.9
H	3 96	63	96	92	96	92	90	84	840	14	59	32	123	151	173	57	16	0	18	0	19	20	22	4.2	12.0	4.9	8.8	3.3	2.9	2.7	25.7	35.2	29.9	28.9	20.8	16.9	16.8
	4 96	43	96	78	90	71	71	68	1810	44	231	106	362	467	524	42	24	5	23	6	26	27	29	3.5	12.5	4.1	8.6	3.3	2.6	2.5	25.2	30.0	25.7	30.0	24.8	14.1	13.9
	5 96	38	96	68	82	62	58	56	2420	87	431	177	534	624	674	37	25	5	22	8	25	28	28	0.9	8.9	1.2	5.2	0.9	0.8	0.7	9.6	24.1	13.2	17.0	9.6	9.2	8.9
	6 96	35	89	62	75	58	59	58	2670	166	601	249	485	523	555	32	28	10	26	16	28	28	28	0.2	7.7	0.2	4.0	0.2	0.2	0.1	2.7	26.1	2.2	17.9	1.8	1.8	1.8

stronger layered graph variants but also exhibits significantly larger LP gaps in our test cases. Thus, it is clearly not competitive to the layered graph approaches. Since in the integer case the latter are additionally expected to benefit much more from built-in preprocessing of state-of-the-art ILP solvers we will not consider model UPath^{DI} in the remainder of this study. Comparing the different layered graph models, the largest improvement on the reported LP gaps is obtained with the inclusion of the directed cutset constraints. On the other hand, their inclusion also significantly increases the runtime. From Table 3 we further observe that when $T' = T \cup R$, that is in the case where the arborescences of each root share the same set of nodes and edges, the addition of equations (23) and (24), often yields a further significant reduction on the reported LP gaps. This reduction is usually obtained with no cost or only with little cost in terms of CPU-time. Adding outdegree constraints (25) for potential Steiner nodes on each layered graph and root-depth constraints (26) further reduces the obtained gaps in many cases. This improvement, however, is typically rather small. On the other hand, since we only dynamically separate these constraints the additional CPU-time is almost negligible.

For $T' = T$, cf. Table 4, we conclude that despite the reported tighter LP bounds, the additional CPU-time needed to solve LG_E is not negligible compared to LG .

Similar to our previous observations w.r.t. LG^{CI} in case $T' = T \cup R$, the bounds of model LG_E^C are clearly better than those of LG_E or LG^C . Outdegree and root-depth constraints produce a further, although usually rather small, improvement on the reported LP bounds. Their influence seems to be more significant for the larger random instances.

Overall, we conclude that the LP gaps usually increase with the instance size, increasing number of root nodes or decreasing hop limit and that the gaps resulting from random instances (R) are usually significantly larger than those resulting from the Euclidean instances (C). Furthermore, all proposed model enhancements are not only of theoretical importance but clearly tighten the LP bounds in many cases. In general the additional CPU-time needed to compute the tighter gaps is reasonable and, as we will see below, using the enhancements often contributes for solving the integer models.

Tables 5 and 6 summarize the computational results for solving the layered graph models in the integer case for $T' = T \cup R$ and $T' = T$, respectively. Here, we report the numbers of instances in each set ($\#$), the numbers of instances solved to proven optimality within the time limit of 7,200 CPU-seconds ($\#_{\text{solved}}$), geometric means of CPU-times in seconds, average optimality gaps in percent, numbers of instances where the the LP relaxation could be solved by each layered graph model ($\#_L$), and average optimality gaps in percent on

them. Hereby, optimality gaps are calculated as $(UB - LB)/UB$ where UB and LB denote the obtained upper and lower bounds, respectively.

From Table 5, i.e., in case $T' = T \cup R$, we first observe that model LG^{CI} clearly outperforms the weaker variants LG and LG^C with respect to all analyzed criteria. Whether LG^{CI} or the two even stronger models LG^{CIO} and LG^{CIOR} perform best heavily depends on the considered instance and its parameters. On the one hand, LG^{CI} often yields the lowest CPU-times and optimality gaps after two hours. On the other hand, LG^{CIO} and LG^{CIOR} successfully solve some instances to proven optimality that could not be solved by the theoretically weaker models. For $T' = T$ the benefit of the stronger models including the various enhancements is intensified. LG_E^{COR} solved more instances to proven optimality than any of the other models. LG_E^C and LG_E^{CO} also perform almost as good. With respect to needed CPU-times, these three models are usually quite close to each other and frequently exhibit a better overall performance than the weaker variants. In particular, we conclude that considering the extended layered graph with $2H - diam(T)$ layers which enables most of the strengthening techniques clearly pays off in practice. When comparing the average gaps grouped by the numbers of root nodes, we observe that only for $|R| = 2$ we were able to solve all instances to optimality. The problem becomes more difficult to solve already for $|R| = 4$, where the average gaps are 11.1% and 21.3% for $T' = T \cup R$ and $T' = T$, respectively. Note that for the instances of manageable size (i.e., where the LP relaxations could be solved by all layered graph models) the average gaps are significantly smaller. When $|R| = 6$ or $|R| = 8$ the remaining gaps remain, however, quite large (e.g., around 26% for $|R| = 8$). Overall, we conclude that the models including the proposed enhancements often outperform their weaker variants and in particular allow to solve more instances to proven optimality within the given time limit.

6. Conclusions

In this article, we studied a generalization of the hop- and diameter constrained Steiner tree problems which arises by introducing multiple central, i.e., root, nodes. After introducing the general case we draw our attention to two particular cases which are motivated from practical applications. For them we identified special polynomially solvable cases and proved that the problem is NP-hard in general. Furthermore, we discussed MIP models for the two cases based on layered graph reformulations together with strengthening valid inequalities, established a hierarchy with respect to their LP relaxation values, and also compared them theoretically to a previously proposed path model. A computational study carried out on

Table 5: Results for $T' = T \cup R$ grouped by instance set, $|R|$, and H . Numbers of instances ($\#_{\text{solved}}$) solved to proven optimality, geometric means of CPU-times in seconds, average optimality gaps in %, numbers of instances ($\#_L$) for which the LP relaxation could be solved by all layered graph variants, and average optimality gaps in % on the them; time limit: 7 200 CPU-seconds.

Set	#	# _{solved}					CPU-time [s]					Avg. Gap [%]					Avg. Gap [%] (LP solved)					
		LG	LG ^C	LG ^{CI}	LG ^{CIO}	LG ^{CIO^R}	LG	LG ^C	LG ^{CI}	LG ^{CIO}	LG ^{CIO^R}	LG	LG ^C	LG ^{CI}	LG ^{CIO}	LG ^{CIO^R}	# _L	LG	LG ^C	LG ^{CI}	LG ^{CIO}	LG ^{CIO^R}
Set	C30 64	48	58	58	59	57	273	79	62	70	72	8.9	5.7	7.9	7.8	10.3	59	6.9	0.8	0.0	1.7	2.7
	C40 64	32	42	48	44	47	1371	417	286	369	355	20.3	21.5	17.5	19.8	20.8	47	8.7	1.4	0.3	3.1	2.6
	C60 64	14	38	38	37	35	4550	1626	1495	1830	1826	42.9	39.1	36.6	38.6	41.7	35	14.7	0.0	0.0	0.0	0.0
	R30 64	58	53	56	58	60	60	86	38	45	44	7.0	13.6	8.3	8.3	6.3	64	7.0	13.6	8.3	8.3	6.2
	R40 64	33	27	33	35	35	698	823	569	574	550	35.2	46.9	39.1	39.0	39.3	56	28.7	39.9	30.7	30.5	30.6
	R60 64	25	23	35	32	31	1597	2007	943	1063	1087	49.2	56.8	39.3	44.5	46.6	43	29.6	37.4	15.1	22.0	22.8
$ R $	2 96	86	93	96	96	96	41	18	11	13	14	1.1	2.1	0.0	0.0	0.0	96	1.1	2.1	0.0	0.0	0.0
	4 96	64	75	84	84	83	702	390	202	254	232	17.3	15.9	9.1	10.0	11.1	92	15.1	15.5	6.2	7.2	7.2
	6 96	37	46	54	52	52	2063	1465	1026	1146	1169	41.7	41.9	33.4	39.0	41.1	68	27.3	23.1	15.1	20.9	21.1
	8 96	23	27	34	33	34	3945	3654	2907	3145	3095	48.9	62.4	56.6	56.3	57.7	48	27.2	33.9	27.4	28.2	26.5
	H	3 96	69	67	77	78	79	300	282	100	118	113	15.4	20.9	10.5	11.3	11.6	92	15.2	19.5	10.6	11.2
4 96	43	49	60	60	58	1052	581	431	472	475	32.3	38.0	29.8	31.1	34.0	77	25.4	27.0	16.8	19.1	20.2	
5 96	48	58	65	63	66	944	546	412	497	500	28.8	34.5	28.6	32.5	30.9	70	11.5	12.3	7.9	10.4	8.1	
6 96	50	67	66	64	62	786	430	370	433	428	32.5	29.1	30.1	30.4	33.5	65	7.6	1.4	1.4	3.1	3.1	

26

Table 6: Results for $T' = T$ grouped by instance set, $|R|$, and H . Numbers of instances ($\#_{\text{solved}}$) solved to proven optimality, geometric means of CPU-times in seconds, average optimality gaps in %, numbers of instances ($\#_L$) for which the LP relaxation could be solved by all layered graph variants, and average optimality gaps in % on the them; time limit: 7 200 CPU-seconds.

Set	#	# _{solved}					CPU-time [s]					Avg. Gap [%]					Avg. Gap [%] (LP solved)									
		LG	LG ^C	LG _E	LG _E ^C	LG _E ^{CO}	LG _E ^{COR}	LG	LG ^C	LG _E	LG _E ^C	LG _E ^{CO}	LG _E ^{COR}	LG	LG ^C	LG _E	LG _E ^C	LG _E ^{CO}	LG _E ^{COR}	# _L	LG	LG ^C	LG _E	LG _E ^C	LG _E ^{CO}	LG _E ^{COR}
Set	C30 64	36	52	42	57	57	56	576	173	370	140	140	143	10.2	15.1	14.5	10.9	10.3	12.5	54	6.9	2.8	7.6	0.0	0.0	0.0
	C40 64	23	35	29	38	38	39	2166	783	1779	834	725	704	26.0	33.1	29.9	33.1	31.6	31.5	39	9.8	2.3	8.5	3.1	1.8	3.1
	C60 64	7	23	9	27	26	27	5581	2631	4930	2854	2905	2912	51.3	56.6	56.1	53.9	51.2	52.6	25	19.0	2.3	18.7	0.0	0.0	0.0
	R30 64	57	50	59	55	54	58	66	104	86	110	96	99	6.4	16.6	2.7	12.9	11.5	7.3	63	6.5	15.4	2.5	11.5	11.7	7.4
	R40 64	26	26	27	30	28	26	980	1103	1082	1018	961	984	45.9	50.2	43.5	47.7	51.0	53.6	48	34.2	40.0	29.9	34.4	36.8	40.2
	R60 64	26	19	26	22	21	23	1792	2180	2205	2475	1954	1911	52.6	63.1	55.0	61.4	61.8	60.2	32	21.5	36.8	18.8	31.7	24.2	24.3
$ R $	2 96	83	93	87	94	95	96	49	22	57	30	24	24	3.0	2.0	2.3	1.3	0.2	0.0	96	3.0	2.0	2.3	1.3	0.2	0.0
	4 96	53	63	60	73	69	71	1082	706	955	693	618	651	19.6	26.8	18.2	20.7	21.9	21.3	82	14.2	19.4	10.9	12.0	11.2	12.5
	6 96	24	34	28	41	41	40	3130	2472	2828	2162	2033	2066	47.3	53.5	50.4	51.4	50.8	52.1	53	28.8	27.7	27.2	26.8	25.5	27.7
	8 96	15	15	17	21	19	22	5258	5145	4956	4591	4614	4456	58.3	74.1	63.6	73.2	72.1	71.6	30	32.9	37.3	28.4	32.6	35.6	26.6
	H	3 96	63	58	64	70	68	70	394	412	366	294	311	306	19.8	25.5	15.2	17.6	18.3	17.9	83	14.6	19.5	11.3	12.4	13.7
4 96	38	43	39	49	50	50	1270	839	1308	885	789	797	33.7	46.4	37.5	47.2	43.8	44.6	68	22.5	29.7	20.5	27.0	22.7	24.7	
5 96	38	47	43	52	51	52	1326	866	1354	945	858	901	34.5	45.1	38.9	43.4	41.1	42.8	54	11.2	11.6	9.1	8.5	7.9	9.0	
6 96	36	57	46	58	55	57	1302	670	1176	827	670	654	40.2	39.5	42.9	38.5	41.8	39.8	56	11.2	1.8	10.5	3.4	4.3	1.8	

a set of benchmark instances known from the literature shows that the branch-and-cut approaches based on the layered graph reformulations clearly outperform the previously leading path model. Our results clearly indicate that all proposed model enhancements reduce the LP gaps in practice. Furthermore, in spite of the additional time needed to solve the LP relaxations, the stronger ILP models often lead to a better overall performance.

The results of our computational study also indicate two directions for potential future research: a) Since even for the strongest among the proposed models the bounds of the linear programming relaxation are sometimes quite large, one may try to identify further strengthening valid inequalities or even different modeling approaches. b) We observed that for several instances, no reasonably good primal solutions could be obtained leading to large optimality gaps. Hence, obtaining high-quality heuristic solutions is another interesting topic for future research. It is, however, an open question whether we can always find a feasible solution to the HSTPMR in polynomial time. We conclude this paper by pointing out that other variants of the more general problem introduced at the beginning of the paper may be worth studying. Consider the variant with $T' = R$ and $V = T \cup R$. This corresponds to the problem of finding a minimum cost spanning tree that includes a diameter constrained Steiner tree with terminal set R . This variant is closely related two-level problem described and studied in [15]. It is also worth pointing out the particular case with $|R| = 2$ where we obtain the problem of finding a minimum cost spanning tree such that the length of the path between the two given root nodes does not exceed H . To the best of our knowledge it is not known and it does not appear to be obvious whether this problem can be solved in polynomial time.

References

- [1] N. R. Achuthan, L. Caccetta, P. A. Caccetta, and J. F. Geelen. Computational methods for the diameter restricted minimum weight spanning tree problem. *Australasian Journal of Combinatorics*, 10:51–71, 1994.
- [2] B. V. Cherkassky and A. V. Goldberg. On implementing push-relabel method for the maximum flow problem. *Algorithmica*, 19:390–410, 1994.
- [3] P. Crescenzi, V. Kann, R. Silvestri, and L. Trevisan. Structure in approximation classes. *SIAM Journal on Computing*, 28:1759–1782, 1999.
- [4] G. Dahl, L. Gouveia, and C. Requejo. On formulations and methods for the hop-constrained minimum spanning tree problem. In Mauricio G. C. Resende and Panos M.

- Pardalos, editors, *Handbook of Optimization in Telecommunications*, pages 493–515. Springer, 2006.
- [5] M. R. Garey and D. S. Johnson. *Computers and Intractability; A Guide to the Theory of NP-Completeness*. W. H. Freeman & Co., 1979.
- [6] L. Gouveia. Using the Miller-Tucker-Zemlin constraints to formulate a minimal spanning tree problem with hop constraints. *Computers & Operations Research*, 22(9):959–970, 1995.
- [7] L. Gouveia and T.L. Magnanti. Network flow models for designing diameter-constrained minimum-spanning and Steiner trees. *Networks*, 41(3):159–173, 2003.
- [8] L. Gouveia and C. Requejo. A new Lagrangian relaxation approach for the hop-constrained minimum spanning tree problem. *European Journal of Operational Research*, 132(3):539–552, 2001.
- [9] L. Gouveia, T.L. Magnanti, and C. Requejo. A 2-path approach for odd-diameter-constrained minimum spanning and Steiner trees. *Networks*, 44(4):254–265, 2004.
- [10] L. Gouveia, T.L. Magnanti, and C. Requejo. An intersecting tree model for odd-diameter-constrained minimum spanning and Steiner trees. *Annals of Operations Research*, 146(1):19–39, 2006.
- [11] L. Gouveia, A. Paias, and D. Sharma. Modeling and solving the rooted distance-constrained minimum spanning tree problem. *Computers & Operations Research*, 35(2):600–613, 2008.
- [12] L. Gouveia, A. Paias, and D. Sharma. Restricted dynamic programming based neighborhoods for the hop-constrained minimum spanning tree problem. *Journal of Heuristics*, 17(1):23–37, 2011.
- [13] L. Gouveia, L. Simonetti, and E. Uchoa. Modeling hop-constrained and diameter-constrained minimum spanning tree problems as Steiner tree problems over layered graphs. *Mathematical Programming*, 128:123–148, 2011.
- [14] L. Gouveia, M. Leitner, and I. Ljubić. On the hop constrained Steiner tree problem with multiple root nodes. In A.R. Mahjoub et al., editors, *Proceedings of the 2nd International Symposium on Combinatorial Optimization*, volume 7422 of *LNCS*, pages 201–212. Springer, 2012.

- [15] L. Gouveia, M. Leitner, and I. Ljubić. The two-level diameter constrained spanning tree problem. Technical Report TR 186–1–12–02, Institute of Computer Graphics and Algorithms, Vienna University of Technology, 2012.
- [16] M. Gruber. *Exact and Heuristic Approaches for Solving the Bounded Diameter Minimum Spanning Tree Problem*. PhD thesis, Vienna University of Technology, Vienna, Austria, 2009.
- [17] I. Ljubić and S. Gollowitzer. Layered graph approaches to the hop constrained connected facility location problem. *INFORMS Journal on Computing*, 2012. to appear.
- [18] I. Ljubić, R. Weiskircher, U. Pferschy, G. Klau, P. Mutzel, and M. Fischetti. An algorithmic framework for the exact solution of the prize-collecting Steiner tree problem. *Mathematical Programming*, 105:427–449, 2006.
- [19] C. Lund and M. Yannakakis. On the hardness of approximating minimization problems. *Journal of the ACM*, 41:960–981, 1994.
- [20] S. Voß. The Steiner tree problem with hop constraints. *Annals of Operations Research*, 86:271–294, 1999.

Appendix

Proof of Lemma 2. $H = 2$: For $|R| \geq 3$, each optimal solution must be a star centered at a node $v \in V$ with all roots and terminals different from v being leaves. Thus, we enumerate all such stars and each one yielding lowest cost is an optimal solution. In case $|R| = 2$ there are additional feasible solutions that can be obtained by assigning each terminal $t \in T$ to the closest of the two roots and connecting the roots by an edge. Thus, we can still obtain an optimal solution by enumeration. This argument holds for both cases, $T' = T$ and $T' = T \cup R$.

$H \geq 3$: To show this non-approximability result, we use an error-preserving reduction (see, e.g. [3]) from the SET COVER problem. Given a set cover instance with the set of elements $X = \{x_1, \dots, x_n\}$ and a collection of subsets $Y = \{y_1, \dots, y_m\}$, we transform it into a HSTPMR instance with two roots 0, 1 and $H = 3$ as follows: Construct a graph G with the set of nodes $V = \{x_1, \dots, x_n, y_1, \dots, y_m, 0, 1\}$. We insert an edge of cost one between x_i and y_j whenever the set y_j contains the element x_i . We connect all y nodes to the root 0 and set the cost of those edges to $n + 1$. Finally, we connect 0 and 1 with

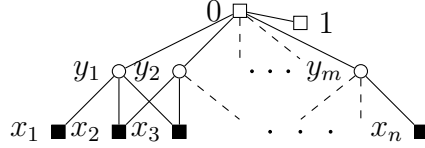


Figure 7: Transformation of a set cover instance with elements $X = \{x_1, \dots, x_n\}$ and subsets $Y = \{y_1, \dots, y_m\}$ to an instance of HSTPMR with $R = \{0, 1\}$, $T = \{x_1, \dots, x_n\}$, and $H = 3$. Edge costs are set to $c_{0y_i} = n + 1$, $1 \leq i \leq m$, $c_{y_i x_j} = 1$, if set y_i , $1 \leq i \leq m$, contains element x_j , $1 \leq j \leq n$, and $c_{01} = 1$.

an edge of cost one. It is not difficult to see that there is a one-to-one correspondence between the set of feasible solutions of the set cover and the set of feasible solutions of the HSTPMR on G with $H = 3$. This transformation can be done in polynomial time. To show that this transformation also preserves the approximation ratio, observe that if the cost of the set cover solution is k , so is the cost of the corresponding HSTPMR solution equal to $F(k) = (n + 1)(k + 1)$. Let S be a feasible HSTPMR solution with the objective value equal to $F(k_s)$ where k_s is the value of the corresponding set cover solution, and let k be the value of the optimal set cover solution. Then we have:

$$\frac{F(k_s) - OPT}{OPT} = \frac{(n + 1)(k_s + 1) - (n + 1)(k + 1)}{(n + 1)(k + 1)} = \frac{k_s - k}{k + 1} \geq \beta \frac{k_s - k}{k}$$

which is true for, e.g., $\beta = 1/2$. Therefore, any approximation algorithm for the HSTPMR that runs in polynomial time cannot have a better approximation ratio than $\Theta(\log n)$ since $\frac{k_s - k}{k} \geq \Theta(\log n)$ holds for the set cover problem unless $P=NP$ [19].

For $|R| \geq 3$, we attach all further roots to 0 and set the edge costs to one. The rest of the proof works similarly.

□

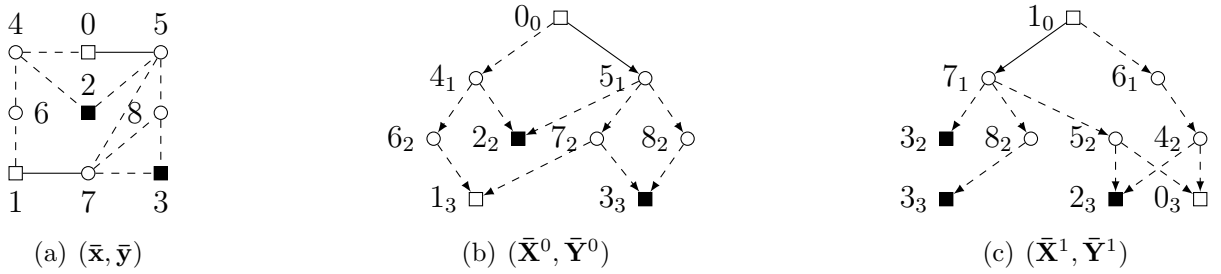


Figure 8: A feasible solution $(\bar{x}, \bar{y}, \bar{X}, \bar{Y})$ to the LP relaxation of LG^C to an instance with $R = \{0, 1\}$, $T = \{2, 3\}$, $T' = T \cup R$, and $H = 3$. (a) Subgraph induced by variable values \bar{x}_e , $e \in E$, and \bar{y}_i , $i \in S$. (b), (c) Subgraphs induced by variable values \bar{X}_{ij}^{sh} , $s \in \{0, 1\}$, $(i_h, j_{h+1}) \in A_L^s$, respectively. Solid (dashed) edges and arcs indicate a corresponding variable value of 1 (0.5); $\bar{y}_5 = \bar{y}_7 = 1$, $\bar{y}_4 = \bar{y}_8 = 0.75$, and $\bar{y}_6 = 0.5$. Observe that arc $(7, 8)$ is used in the arborescences rooted at 1 but neither arc $(7, 8)$ nor arc $(8, 7)$ can be part of a feasible arborescence rooted at 0 since potential Steiner nodes do not exist at layer H , i.e., $i_H \notin V_L^s$, $\forall i \in S$, $\forall s \in R$. Similarly, arc $(5, 8)$ is used in the arborescence rooted at 0 but neither $(5, 8)$ nor $(8, 5)$ can be part of a feasible arborescence rooted at 1. Further note, that in order to satisfy constraints (3)–(5) the unique feasible assignment of node variable values is $\bar{y}_5 = \bar{y}_7 = 1$, $\bar{y}_4 = \bar{y}_8 = 0.75$, and $\bar{y}_6 = 0.5$ and it is not possible to derive feasible arborescences on the layered graphs such that $\sum_{h=1}^{H-1} \bar{Y}_i^{sh} = y_i$, $\forall s \in R$, $\forall i \in S$.

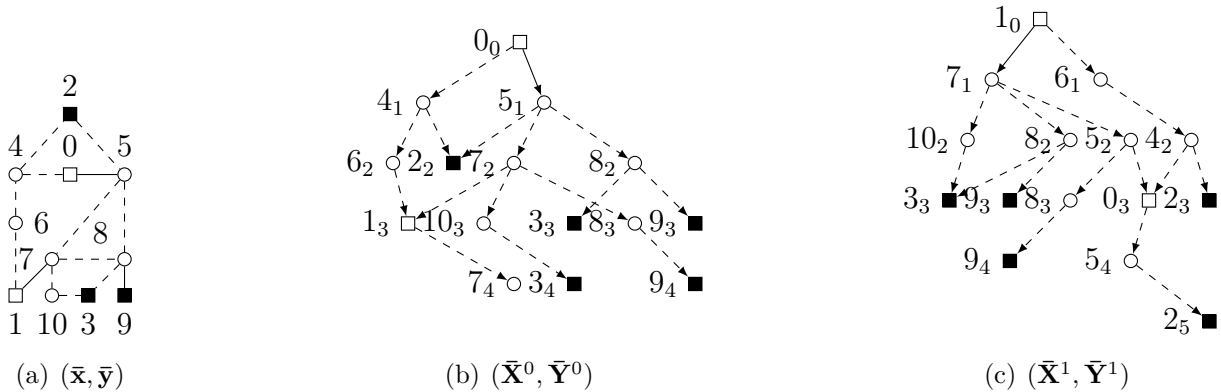


Figure 9: A feasible solution $(\bar{x}, \bar{y}, \bar{X}, \bar{Y})$ to the LP relaxation of LG^{CI} to an instance with $R = \{0, 1\}$, $T = \{2, 3, 9\}$, $T' = T \cup R$, and $H = 5$. (a) Subgraph induced by variable values \bar{x}_e , $e \in E$, and \bar{y}_i , $i \in S$. (b), (c) Subgraphs induced by variable values \bar{X}_{ij}^{sh} , $s \in \{0, 1\}$, $(i_h, j_{h+1}) \in \hat{A}_L^s$, respectively. Dashed (solid) edges and arcs indicate a corresponding variable value of $1/2$ (1); $\bar{y}_4 = \bar{y}_6 = \bar{y}_{10} = 0.5$, and $\bar{y}_i = 1$, $i \in \{5, 7, 8\}$. This solution clearly violates inequalities (25) since Steiner node 7 is a leaf in the arborescence on G_L^0 . Further note, that for the given values of \bar{x} and \bar{y} each feasible set of arborescences must contain Steiner nodes as leaves to satisfy constraints (23) and (19), i.e., the solution cannot satisfy inequalities (25).